Forward Laser Plasma Accelerator for Relativistic Plasma Propulsion

IEPC-2007-96

Sota Sumida[*], Masakuni Takagi[†], Hideyuki Horisawa[‡]
Tokai University, Hiratsuka-shi, Kanagawa, 259-1292, Japan

Ikkoh Funaki[§]
Japan Aerospace Exploration Agency , Sagamihara, Kanagawa, 229-8510, Japan

Itsuro Kimura[**]
University of Tokyo, Bunkyo-ku, Tokyo, 113-8856, Japan

Abstract: Fundamental investigations on fast ion emission characteristics from a laser-plasma accelerator employing laser-foil interactions were conducted using a PIC code. From the results, it was shown that particles were accelerated in the direction of the incident laser beam. Some parts of the electric and charged particle waves inside the target were decreased in their amplitudes and distorted having nonlinear components. Moreover, it was confirmed that higher order of harmonic wave components of the incident wave of the laser beam were generated in the target. One of the acceleration mechanisms is probably as follows. The particles were first accelerated inducing velocity in the vertical direction by the vertical electric field of the incident laser beam. At the same time, with the interaction of the velocity and the horizontal magnetic field of the laser beam, the particles were accelerated to the axial direction. Through this process, the particles are given the kinetic energy or accelerated into vacuum.

I. Introduction

THE interaction of ultraintense laser pulses with solid targets leads to generation of fast particles, from x- and γ-ray photons to high energy ions, electrons, and positrons.[1–9] In particular, an interest has developed in ion acceleration by compact high-intensity femtosecond lasers with potential applications for the initiation of nuclear reactions on a tabletop. Experiments now being carried out involve high energy ions generated in the interaction of laser pulses with solid thin-film targets as shown in Fig.1. In this case, strong electrostatic fields can be generated through charge separation. This phenomena is dominated by laser energy. Thermal expansion of the laser-driven plasma and ponderomotive electron expulsion constitute the most well-known examples of the electrostatic-fields production (Fig.1)[9].

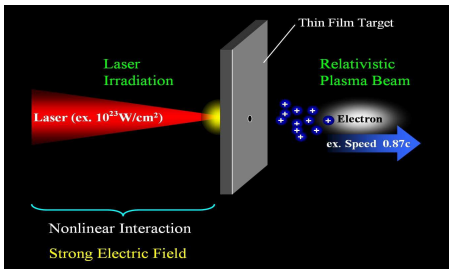

Fig 1.Schematic image of forward laser plasma acceleration through laser-target interaction.

[*] Graduate Student, Department of Aeronautics and Astronautics, sota@isas.jaxa.jp
[†] Graduate Student, Department of Aeronautics and Astronautics, 6amjm016@tokai.ac.jp
[‡] Associate Professor, Department of Aeronautics and Astronautics, horisawa@tokai.ac.jp
[§] Associate Professor, Institute of Space and Astronautical Science, funaki@isas.jaxa.jp
[**] Professor Emeritus, University of Tokyo

Table 1. Plasma accelerators by an intense laser pulse (λ_L : wavelength of the laser pulse, E_L: pulse energy, τ_L : pulse width, P_L: peak power, I_L: laser intensity, E_{ion}: accelerated ion energy, N_{ion}: number of ions, u_{ion}: velocity of ions, c: speed of the light, I_{sp}: specific impulse).

Laboratory	λ_L [μm]	E_L [J]	τ_L [psec]	P_L [W]	I_L [W/cm^2]	Ions (Target)	E_{ion} [MeV]	N_{ion} /pulse	E_{ion}/E_L	(u_{ion}/c)	I_{sp} [Msec]
RAL	1.053	30	1.8 ~ 4	–	2×10^{18}	Proton (Mylar disk)	4.2 (1.3)[b]	–	0.1	0.094	2.899
RAL	1.053	30	~ 1	–	10^{19}	Proton (CH disk)	12 (1 ~)	–	–	0.158	4.910
RAL	1.053	50	0.9 ~ 1.2	–	5×10^{19}	Proton (Al foil)	18 (2 ~)	10^{12}	(0.06)[b]	0.193	6.022
LLNL	1.053	< 1k	0.45	~ 10^{15}	6×10^{20}	Proton (Metal foil)	50	–	–	0.317	10.12
LLNL	1.000	–	0.5, 5	~ 10^{15}	3×10^{20}	Proton (Plastic CH)	55 (10 ~)	3×10^{13}	0.06	0.327	10.63
LLNL	1.000	–	0.5	~ 10^{15}	3×10^{20}	Proton (CH polymer)	58 (10 ~)	2×10^{13}	0.12	0.336	10.92
LLNL	0.400	–	0.01 ~ 0.2	~ 10^{15}	10^{18} ~ 10^{22}	Proton (Al, CH foil)	29	3×10^{13}	0.2	0.243	7.667
Osaka U.	1.000	–	0.018	~ 10^{15}	1.6×10^{22}	Proton (Plasma slab)	~ 1000	–	–	0.875	55.29

To apply this phenomenon to space propulsion system, a collimated plasma beam will be preferable. The collimation requires a planer charge separation, which can be achieved by focusing an intense laser pulse onto the surface of a planar solid-density film. In this case the laser light terminates at the target surface and high-energy electrons generated in front of it deep inside the target. These electrons produce a strong electrostatic field accelerating ions in a forward direction. High energy electrons expand faster and the ions form a well collimated beam confined in the transverse direction by the pinching in the self-generated magnetic field. The ions in the beam expand in the longitudinal direction because the electric charge is not compensated inside. It has been shown that the mechanism of this anisotropic Coulomb explosion is at work in the case of the interaction of a petawatt laser with a thin slab of overdense plasma and accelerates ions up to relativistic energies. The electromagnetic filamentation instability leads to magnetic pinching in the transverse direction and to collimated beam formation.

Recent experimental and theoretical results of laser plasma accelerators in various laboratories are listed in Table 1. Maximum ion energy of order tens of MeV through the acceleration has been reported in recent studies, are also added.[10,11] From the table, as for a proton beam accelerated up to 58 MeV, its speed corresponds to 33 % of the speed of light and the specific impulse Isp of order 10^7 sec. Moreover, in theoretical studies, it was predicted that the relativistic ion beam, $u_{ion}/c \sim 87$ % and specific impulse $I_{sp} \sim 0.55 \times 10$ sec, is achievable with current laser facilities.[5]

Although those accelerators were originally developed for the use of igniters for nuclear fusion reactions, we propose the use for space propulsion applications.[10–12] For the propulsion applications based on the relativistic beams, extremely high values of the specific impulse can be expected through the relativistic effects.[10,11] In cases of operations of this type of thrusters on earth and/or in the solar orbit, in which solar power is available, the merit of high specific impulse will bring about a significant advantage. The use of this type of propulsion system may also bring some solutions to the problem of the inherent penalty of extremely large mass of propellant required in interstellar flight missions.[10–13]

Since no special nozzle or channel but only a thin film target is needed for the collimated plasma beam formation as shown in Fig.1, the propulsion system employing this technique can be significantly simple and small. In this study, a preliminary investigation is conducted on characteristics of plasmas induced in the forward laser plasma acceleration with a nanosecond laser. Since no special nozzle or channel but only a thin film target is needed for the collimated plasma beam formation as shown in Fig.1, the propulsion system employing this technique can be significantly simple and small. In this study, a preliminary investigation is conducted on characteristics of plasmas induced in the forward laser plasma acceleration with a nanosecond laser.

II. PIC (Particle-In-Cell) Simulation

A preliminary PIC (particle-in-cell) simulation was conducted to investigate the acceleration mechanisms of laser-film interaction. In Fig. 2, simulation model is shown. Assuming a planar electromagnetic wave, having the vertical electric field component E_y and the horizontal magnetic field component B_z, as a laser beam, which impinges to a thin solid film and penetrates into it, a 1-dimensional (or 1.5-D) simulation considering Aluminum particle motion in x-direction was conducted.

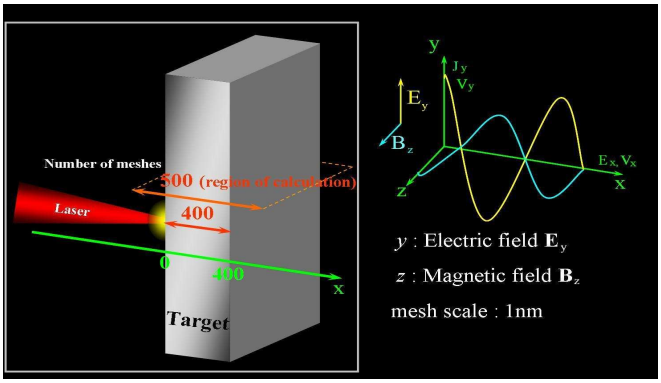

Fig. 2. Simulation model

A. Temporal Behaviors of Particles and Electromagnetic Wave

Temporal evolutions of the vertical electric field of an incident laser pulse and the x-component velocity of the particles, which are electrons in these cases, at an initial phase of 0.5 to 2.5 fsec after laser irradiation for the laser intensity I_L = 2.7 x 10^{17} W/cm^2, wavelength λ_L = 100 nm, target thickness t = 400 nm are shown in Fig.3. In this figure, positions of top and bottom surfaces of the target are indicated as dotted lines. At 0.5 fsec at which only one wavelength of the laser beam is penetrating into the target, electric field strength is slightly reduced inside the target. At the same time, particles inside the target at one wavelength depth are accelerated gaining axial velocity, or x-component velocity of about 8 % of the speed of light at maximum ((d) and (e)). After 1.5 fsec at which the laser wave is emitted from the bottom surface of the target, its field strength is decreased down to about 50 % ((b) and (c)). Then bunch of the particles start jumping out from the bottom surface, or being accelerated into the vacuum ((e) and (f)). As can be seen in (f), the maximum velocity of the accelerated particles is about 11 % of the speed of light in this case.

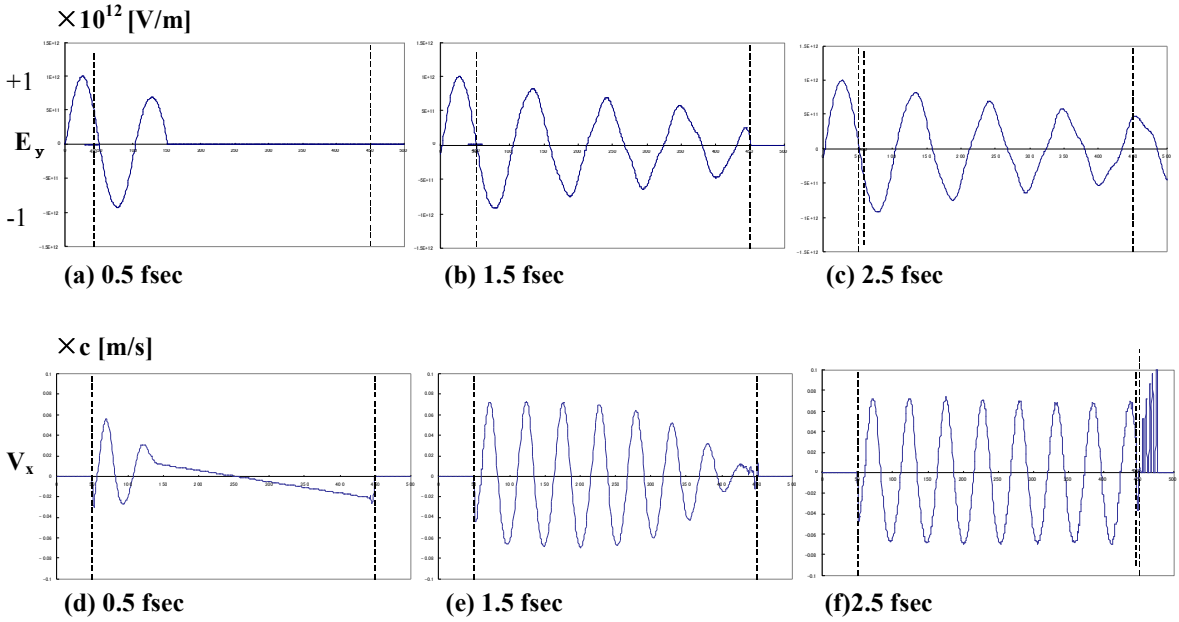

Fig. 3. Temporal evolution of vertical electric field E_y and axial velocity V_x for Laser intensity I_L = 2.7 x 10^{17} W/cm^2, wavelength λ_L = 100 nm, target thickness t = 400 nm.

Temporal evolutions of the vertical electric field and axial velocity of the particles at an initial phase for the higher laser intensity I_L = 6.8 x 10^{17} W/cm^2, wavelength λ_L = 100 nm, target thickness t = 400 nm are shown in Fig.4. Although temporal behaviors of the electric field and the particles are similar to the lower intensity case in Fig.3, particles inside the target at one wavelength depth at 0.5 fsec are gaining axial velocity of about 10 % of the speed of light at maximum ((d) and (e)). After 1.5 fsec at which the laser wave is emitted from the bottom surface of the target, its field strength is decreased down to about 30 % ((b) and (c)). Then bunch of the particles are accelerated into the vacuum ((e) and (f)). As can be seen in (f), the maximum velocity of the accelerated particles is about 18 % of the speed of light in this case.

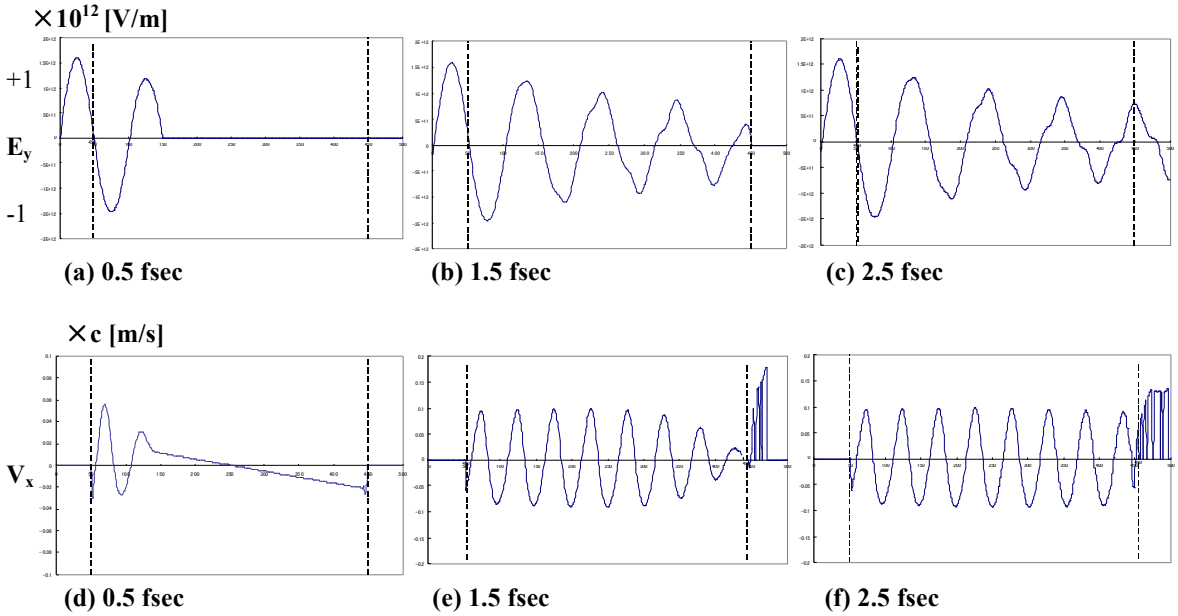

Fig. 4. Temporal evolution of vertical electric field E_y and axial velocity V_x for Laser intensity I_L = 6.8 x 10^{17} W/cm^2 , wavelength λ_L = 100 nm, target thickness t = 400 nm.

B. Acceleration mechanism

In (e) and (f) of Figs.3 and 4, the particle motion in axial direction inside the target is occurring at positions where electric field gradients taking the maximum values. Inside the target, the particles are having oscillating velocities for forward and backward directions with their wavelength of a half of the incident laser wave. Also it can be seen that these particle motions or waves are in phase with the incident laser beam. At the bottom surface and outside the target, particles are being accelerated only in the forward direction having higher velocities than those of inside the target. From these results, it was confirmed that particles were being accelerated in phase, or on the wave, with the incident laser beam.

In (b) and (c) of Figs.3 and 4, it can be seen that some parts of the electric wave inside the target are decreased in their wave heights and distorted in their wave shapes having nonlinear components. From the spectral analysis, it was confirmed that most of the components was the third harmonic wave of the incident wavelength of the laser beam. Through this process including the nonlinear phenomena, particles are given the kinetic energy or accelerated into vacuum.

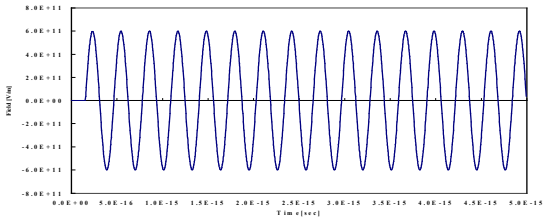

(a) E_y at x=0

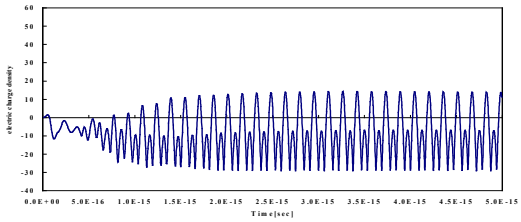

(b) Charge Density at x=0

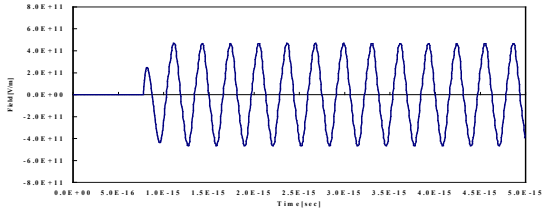

(c) E_y at x=200

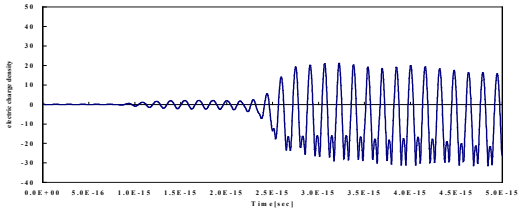

(d) Charge Density at x=200

Fig. 5. Temporal variation of electric field *E*y and charge density of 0 to 5.0 fsec at arbitrary place. Laser intensity I_L = 0.6 x 10^{12} W/cm^2, wavelength λ_L = 100 nm, target thickness *t* = 400 nm

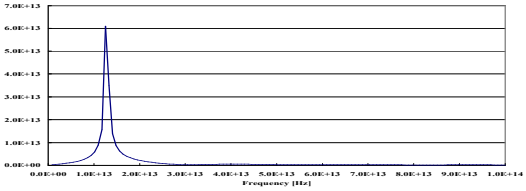

(a) x=0 Electric Field (FFT)

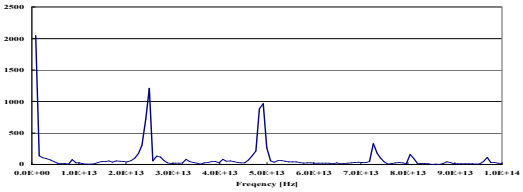

(b) x=0 Electric Charge Density (FFT)

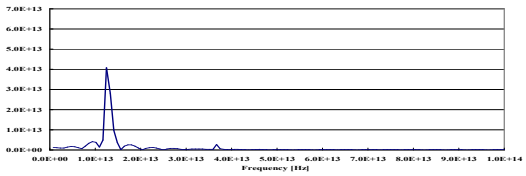

(c) x=200 Electric field (FFT)

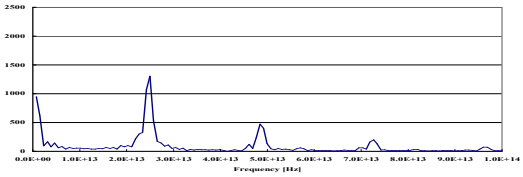

(d) x=200 Electric Charge density (FFT)

Fig. 6. Spectra of electric-field wave and charge density wave transferred from Fig.5.

possible contributing the particle acceleration are as follows; at first, the particles are accelerated to vertical- or *y*-direction inducing velocity in *y*-direction V_y by the vertical electric field E_y of the incident laser beam. At the same time, with interaction of the vertical velocity V_y and horizontal magnetic field B_z of the laser beam, or Lorentz force $F_x = qVB$, the particles are accelerated to *x*-direction.

Temporal variations of the electric field and the charge density at typical positions, at target surface and at middle point inside the target, are shown in Fig.5, and their Fourier transferred spectra are given in Fig.6. It can be seen that the higher order harmonic waves of charged particle motion, which are electrons in this case, are being induced at the target surface, although distortion of the incident electromagnetic wave, or electric wave, is insignificant. At the middle point, the amplitude of the electric wave becomes lower, and at the arrival of the electric wave charged particles start shaking. At about 2 fsec after the arrival of the electric wave, the amplitude of oscillation of the charged particles abruptly becomes larger than before. At this point, the higher order harmonic waves of charged particle motion are taking place at the same time.

The mechanism of the formation of such nonlinear phenomena is very complicated. One of which is probably due to the above mentioned Lorentz force induced through the interaction of the *y*-component-velocity of charged particle with the horizontal magnetic field of the incident electromagnetic wave, accelerating particles into *x*-direction. As the amplitude of oscillation, or velocity, in *y*-direction becomes greater at this time, the Lorentz force becomes stronger causing motion of the particles in *x*-*y* plane.

III. Conclusion

Fundamental investigations on fast ion emission characteristics from a laser-plasma accelerator employing laser-foil interactions were conducted using a PIC code. From the results, it was shown that particles were accelerated in the forward direction of the incident laser beam. Some parts of the electric and charged particle waves inside the target were decreased in their amplitudes and distorted having nonlinear components. Moreover, it was confirmed that higher order of harmonic wave components of the incident wave of the laser beam were generated in the target. One of the acceleration mechanisms is probably as follows. The particles were first accelerated inducing velocity in the vertical direction by the vertical electric field of the incident laser beam. At the same time, with interaction of the velocity and the horizontal magnetic field of the laser beam, particles were accelerated to axial direction. Through this process, particles are given the kinetic energy or accelerated into vacuum.

References

[1] Fews, A.P., Norreys, P.A., Beg, F.N., Bell, A.R., Dangor, A.E., Danson, C.N., Lee, P., and Rose, S.J., "Plasma Ion Emission from High Intensity Picosecond Laser Pulse Interactions with Solid Targets," *Physical Review Letters* Vol.73, No.13, 1994, pp.1801-1804.

[2] Lawson, W.S., Rambo, P.W., and Larson, D.J., "One Dimensional Simulations of Ultrashort Intense Laser Pulses on Solid-Density Targets," *Physics of Plasmas*, Vol.4, No.3, 1997, pp.788-795.

[3] Beg, F.N., Bell, A.R., Dangor, A.E., Danson, C.N., Fews, A.P., Glinsky, M.E., Hammel, B.A., Lee, P., Norreys, P.A., and Taterakis, "A Study of Picosecond Laer-Solid Interactions up to 1019 W cm-2," *Physics of Plasmas*, Vol.4, No.2, 1997, pp.447-457.

[4] Roth, M., Cowan, T.E., Hunt, A.W., Johnson, J., Brown, C., Fountain, W., Hatchett, S., Henry, E.A., Key, M.H., Kuehl, T., Parnell, T., Pennington, D.M., Perry, M.D., Sangster, T.C., Christl, M., Singh, M., Snavely, R., Stoyer, M., Takahashi, Y., and Wilks, S.C., "High-Energy Electron, Positron, Ion and Nuclear Spectroscopy in Ultra-Intense Laser-Solid Experiments on the Petawatt," *First International Conference on Inertial Fusion Science and Application*s, 1999.

[5] Sentoku, Y., Liseikina, T.V., Esirkepov, T. Zh., Califano, F., Naumova, N.M., Ueshima, Y., Vshikov, V.A., Kato, Y., Mima, K., Nishihara, K., Pegoraro, F., and Bulanov, S.V., "High Density Collimated Beams of Relativistic Ions Produced by Petawatt Laser Pulses in Plasmas," *Physical Review E*, Vol.62, No.5, 2000, pp.7271 – 7281.

[6] Clark, E.L., Krushelnick, K., Davis, J.R., Zepf, M., Tatarakis, M., Beg, F.N., Machacek, A., Norreys, P.A., Santala, M.I.K., Watts, I., and Dangor, A.E., "Measurements of Energetic Proton Transport through Magnetized Plasma from Intense Laser Interactions with Solids," *Physical Review Letters*, Vol.84, No.4, 2000, pp.670-673.

[7] Hatchett, S.P., Brown, C.G., Cowan, T.E., Henry, E.A., Johnson, J.S., Key, M.H., Koch, J.A., Langdon, A.B., Lasinski, B.F., Lee, R.W., Mackinnon, A.J., Pennington, D.M., Perry, M.D., Phillips, T.W., Roth, M., Stangster, C., Singh, M.S., Snavely, R.A., Stoyer, M.A., Wilks, S.C., and Yasuike, K., "Electron, Photon, and Ion Beams from the Relativistic Interaction of Petawatt Laser Pulses with Solid Targets," *Physics of Plasmas*, Vol.7, No.5, 2000, pp.2076-2082.

[8] Snavely, R.A., Key, M.H., Hatchett, S.P., Cowan, T.E., Roth, M., Phillips, T.W, Stoyer, M.A., Henry, E.A., Sangster, T.C., Singh, M.S., Wilks, S.C., MacKinnon, A., Offenberger, A., Pennington, D.M., Yasuike, K., Langdon, A.B., Lasinski, B.F., Johnson, J., Perry, M.D., and Campbell, E.M., "Intense High-Energy Proton Beams from Petawatt-Laser Irradiation of Solids," *Physical Review Letters*, Vol.85, No.14, 2000, pp.2945-2948.

[9] Maksimchuk, A., Gu, S., Flippo, K., Umstadter, D., and Bychenkov, V., Yu.,"Forward Ion Acceleration in Thin Films Driven by a High-Intensity Laser," *Physical Review Letters*, Vol.84, No.18, 2000, pp.4108-4111.

[10] Horisawa, H., and Kimura, I., "Characterization of Novel Laser Particle Accelerators for Space Propulsion," AIAA 2000-3487 (2000).

[11] Horisawa, H., and Kimura, I., "Laser Plasma Accelerator for Space Propulsion," AIAA 2001-3662 (2001).

[12] Horisawa, H., Kuramoto, H., Oyaizu, K., Uchida, N., and Kimura, I., "Fundamental Study of a Relativistic Laser-Accelerated Plasma Thruster," *Beamed Energy Propulsion: First Intl. Symp. Beamed Energy Propulsion*, 2003, pp.411–422.
[13] Kammash, T. "Advanced Space Propulsion with Ultra-Fast Lasers," *Beamed Energy Propulsion: First Intl. Symp. Beamed Energy Propulsion*, 2003, pp.411–422.
[14] Stuhlinger E., *Ion Propulsion for Space Flight*, McGraw-Hill (1964).
[15] Kimura, I., *Rocket Engineering*, Yokendo (1993) (in Japanese).
[16] Birdsall, C. K., and Langdon, A. B., *Plasma Physics via Computer Simulation*, Adam Hilger (1991).
[17] The NIST spectra Line Database, http://physics.nist.gov/cgi-bin/atData/main_asd.
[18] Weaver, I., Martin, G. W., Graham, W. G., Morrow, T., and Lewis, C. L. S., "The Langmuir Probe as a Diagnostic of the Electron Component within Low Temperature Laser Ablated Plasma Plumes," *Review of Scientific Instruments*, Vol.70, No.3, 1999, pp.1801–1805.